nature medicine

NKCC1 transporter facilitates seizures in the developing brain

Volodymyr I Dzhala[1,5], Delia M Talos[2,5], Dan A Sdrulla[1], Audrey C Brumback[1], Gregory C Mathews[3], Timothy A Benke[1], Eric Delpire[4], Frances E Jensen[2] & Kevin J Staley[1]

During development, activation of Cl^--permeable $GABA_A$ receptors ($GABA_A$-R) excites neurons as a result of elevated intracellular Cl^- levels and a depolarized Cl^- equilibrium potential (E_{Cl}). GABA becomes inhibitory as net outward neuronal transport of Cl^- develops in a caudal-rostral progression. In line with this caudal-rostral developmental pattern, GABAergic anticonvulsant compounds inhibit motor manifestations of neonatal seizures but not cortical seizure activity. The Na^+-K^+-$2Cl^-$ cotransporter (NKCC1) facilitates the accumulation of Cl^- in neurons. The NKCC1 blocker bumetanide shifted E_{Cl} negative in immature neurons, suppressed epileptiform activity in hippocampal slices *in vitro* and attenuated electrographic seizures in neonatal rats *in vivo*. Bumetanide had no effect in the presence of the $GABA_A$-R antagonist bicuculline, nor in brain slices from NKCC1-knockout mice. NKCC1 expression level versus expression of the Cl^--extruding transporter (KCC2) in human and rat cortex showed that Cl^- transport in perinatal human cortex is as immature as in the rat. Our results provide evidence that NKCC1 facilitates seizures in the developing brain and indicate that bumetanide should be useful in the treatment of neonatal seizures.

Neonatal seizures are potentially catastrophic conditions affecting infants in the first 28 d of life[1]. Their appearance may portend severe neurological dysfunction[2–4]. Both clinical and experimental studies indicate that neonatal seizures lead to long-term impairments in brain development and seizure threshold[5–9]. Neonatal seizures are difficult to treat, and even when the clinical manifestations are suppressed, electroencephalographic (EEG) recordings show ongoing cortical seizure activity[10,11].

GABA is the primary inhibitory neurotransmitter in adult mammalian brain. But in neonates, activation of Cl^--permeable $GABA_A$-Rs excites many neurons[12,13], and this has been linked to a higher propensity for seizures[14,15]. Developing neurons mature in their GABA signaling in a caudal-rostral direction[16]. This provides a potential mechanism for the clinical observation that barbiturates and benzodiazepines, drugs that increase the effects of GABA, suppress the motor component of neonatal seizures, presumably by increasing GABA-mediated inhibition in the spinal cord and brainstem, but do not suppress the EEG seizures because of the persistent excitatory effects of GABA in more rostral structures[10,11,17].

The excitatory action of GABA depends on an elevated intracellular Cl^- level and a depolarized Cl^- equilibrium potential (E_{Cl})[18]. Neonates accumulate Cl^- through the action of the Na^+-K^+-$2Cl^-$ cotransporter (NKCC1, encoded by *SLC12A2*)[19–21], which is exquisitely sensitive to the diuretic bumetanide[22,23]. *SLC12A2* mRNA expression level is high in early postnatal days, but decreases during postnatal development, whereas expression of mRNA encoding the Cl^--extruding K^+-Cl^- cotransporter (KCC2) shows the opposite pattern[21,24,25]. Developmental upregulation of KCC2 expression is considered to promote the switch from excitatory to fast inhibitory action of GABA[26,27]. We tested the hypothesis that in the immature brain, before physiological expression of KCC2, alteration of the ionic basis for GABA-mediated excitation by diuretic drugs inhibits seizure activity in the immature brain. NKCC1 blockade by the diuretic bumetanide inhibits seizure activity *in vitro* and *in vivo* by enhancing GABA-mediated inhibition through blockade of Cl^- uptake by NKCC1. Notably, because of the unique sensitivity of NKCC1 to bumetanide[23], this agent is effective at dosages that have already been extensively tested in human neonates in studies of diuretic drugs[28,29]. Furthermore, we show that NKCC1 is highly expressed in both rat and human cortex during the neonatal period.

RESULTS

High NKCC1 expression in developing cortical neurons

Previous studies have shown that, unlike the adult brain, the developing rodent brain is characterized by increased NKCC1 expression, and associated with low KCC2 levels[24,25,30]. We hypothesized that expression of NKCC1 and KCC2 may be similarly developmentally regulated in the human neocortex, contributing to increased seizure susceptibility in neonates and relative refractoriness of neonatal seizures to GABA agonists. We analyzed the expression level of

[1]Departments of Neurology and Pediatrics, School of Medicine, University of Colorado Health Sciences Center, 4200 East Ninth Avenue, Denver, Colorado 80262, USA. [2]Department of Neurology, Children's Hospital, Harvard Medical School, 300 Longwood Avenue, Boston, Massachusetts 02115, USA. [3]Department of Anesthesiology, Vanderbilt University Medical Center, 6140 MRB III, 465 21st Avenue South, Nashville, Tennessee 37232-8552, USA. [4]Department of Neurology, Vanderbilt University Medical Center, MRB III, T-4202 MCN 2520, Nashville, Tennessee 37232-8552, USA. [5]These authors contributed equally to this work. Correspondence should be addressed to K.J.S. (kevin.staley@uchsc.edu).

Received 4 April; accepted 24 August; published online 9 October 2005; doi:10.1038/nm1301

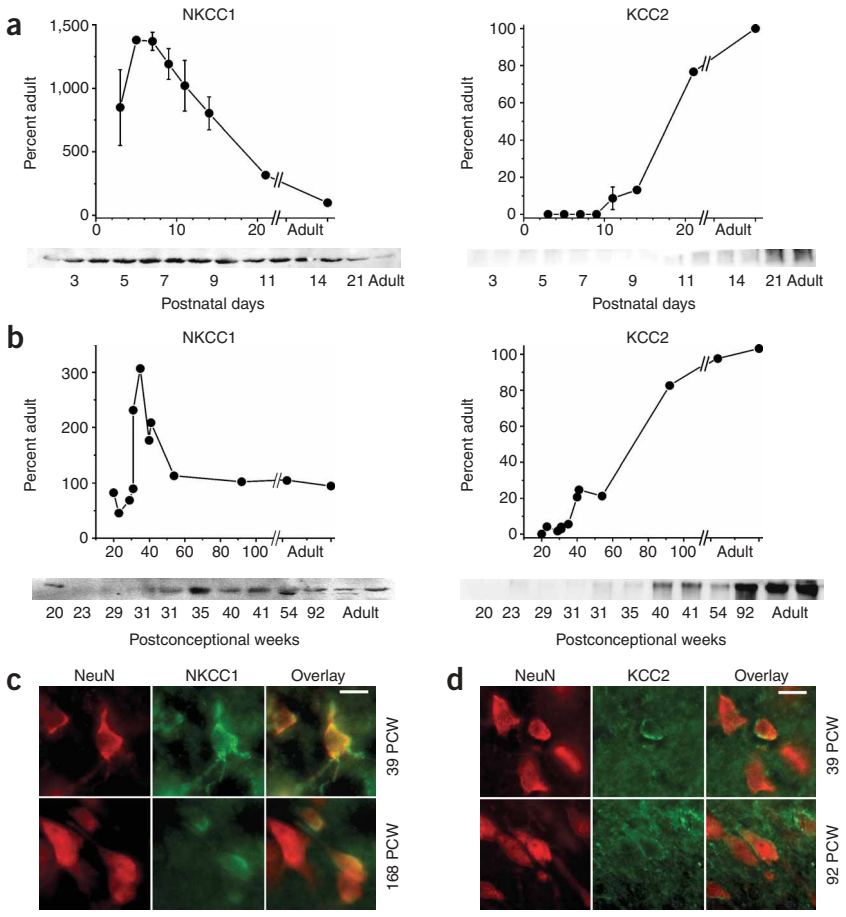

Figure 1 Developmental regulation of NKCC1 and KCC2 in perinatal rat and human cortex. Immunolocalization of NKCC1 and KCC2 in the human neocortex. (**a**) NKCC1 (left) and KCC2 (right) protein quantification in rat cortex, expressed as a percentage of adult levels, at different postnatal ages. Insets are corresponding western blots. (**b**) NKCC1 (left) and KCC2 (right) protein levels in human parietal cortical tissue, as a percentage of adult expression, from midgestation (20 PCW) through adulthood (38–57 years). Insets are corresponding western blots. (**c**) NKCC1 expression pattern in human parietal cortical neurons at term birth versus early childhood. NKCC1 is highly expressed on layer V cortical pyramidal neurons at 39 PCW, whereas at 168 PCW (2.5 years) pyramidal neurons show low or no NKCC1 expression. Immunofluorescence double labeling was performed with neuron-specific marker NeuN (red) and NKCC1-specific antibodies (green). Scale bar, 20 μm. (**d**) KCC2 expression pattern in human parietal cortical neurons at term birth versus early childhood. KCC2 immunoreactivity is seen only in scattered neurons at 39 PCW, in contrast to intense KCC2 labeling on the majority of layer V pyramidal neurons at 92 PCW (1 year). Immunofluorescence double labeling was performed with neuron-specific marker NeuN (red) and KCC2-specific antibodies (green). Scale bar, 20 μm.

NKCC1 and KCC2 in both rat and human cortex by western blot and immunofluorescence double labeling.

Developmental regulation of NKCC1 and KCC2 in rat cortex

Western blot analysis of rat cortical tissue showed a distinct pattern of developmental expression for each transporter. NKCC1 expression was significantly higher between postnatal day (P)3–P14 than at P21 and in adulthood ($P < 0.01$), and peaked at approximately 14-fold higher levels than in the adult (**Fig. 1a**). In contrast, KCC2 levels were significantly lower during the first two postnatal weeks (P3–14) than at P21 and adulthood ($P < 0.001$; **Fig. 1a**). Immunofluorescence double labeling with the neuronal marker NeuN and either NKCC1-specific or KCC2-specific antibodies confirmed the ontogeny shown by western blots. Between P3 and P11, NKCC1 was highly expressed in most cortical neurons, whereas at P14 and P21 there was a considerable decrease in neuronal NKCC1 expression (data not shown). During the entire developmental window analyzed, we also observed NKCC1 protein in non-neuronal cells, located predominantly in the deep cortical layers and subcortical white matter. We first detected KCC2 expression around P7 and it was limited to a few neurons scattered throughout the cortex. We observed a modest increase in the number of KCC2-expressing neurons at P14, whereas at P21 the majority of cortical neurons were intensely labeled on both cell bodies and processes.

Age-specific expression of NKCC1 and KCC2 in human cortex

There were notable similarities in the developmental expression pattern of both transporters between rat and human. At 31–41 postconceptional weeks (PCW), NKCC1 expression was significantly higher than at 1 year (or 92 PCW) and older ($P < 0.03$), peaking at approximately threefold higher at 35 PCW (**Fig. 1b**). During the first year of life (54 and 92 PCW), NKCC1 expression rapidly decreased to levels of the adult. We observed a different expression pattern for KCC2. During the entire fetal and neonatal period (20–41 PCW), KCC2 expression was significantly lower than in adult ($P < 0.001$). Between 31 and 41 PCW, when NKCC1 levels were peaking, KCC2 expression was approximately 2–25% of adult levels, rising over the first year of life (**Fig. 1b**). Immunofluorescence double labeling with neuronal marker NeuN and antibodies to NKCC1 and KCC2 was consistent with the western blot results. Between 31 and 45 PCW, the majority of cortical neurons showed robust NKCC1 immunoreactivity on cell bodies and processes, whereas during early childhood (92–210 PCW, approximately 1–3.3 years) both the number of labeled neurons, as well as the staining intensity, decreased considerably (**Fig. 1c**). We also observed non-neuronal NKCC1 expression, mostly in the subcortical white matter. In contrast, we saw KCC2 expression exclusively in neurons. At younger ages (31–45 PCW), only scattered cortical neurons were labeled with KCC2-specific antibody and the very punctuate staining was weak and limited to the cell body. At older ages (92–210 PCW, or 1–3.3 years), the majority of neurons showed intense KCC2 immunoreactivity on both cell bodies and proximal dendrites (**Fig. 1d**). These data suggest that, as in the rodent, expression of the Cl^- transporter in perinatal human cortex would result in high intracellular Cl^- that in turn could contribute to GABA-mediated excitation and/or a poor response of neonatal seizures to GABAergic anticonvulsants[31].

Low efficacy of phenobarbital in developing hippocampus

The most commonly used medical treatments for neonatal seizures, phenobarbital and benzodiazepines, increase $GABA_A$-R–mediated

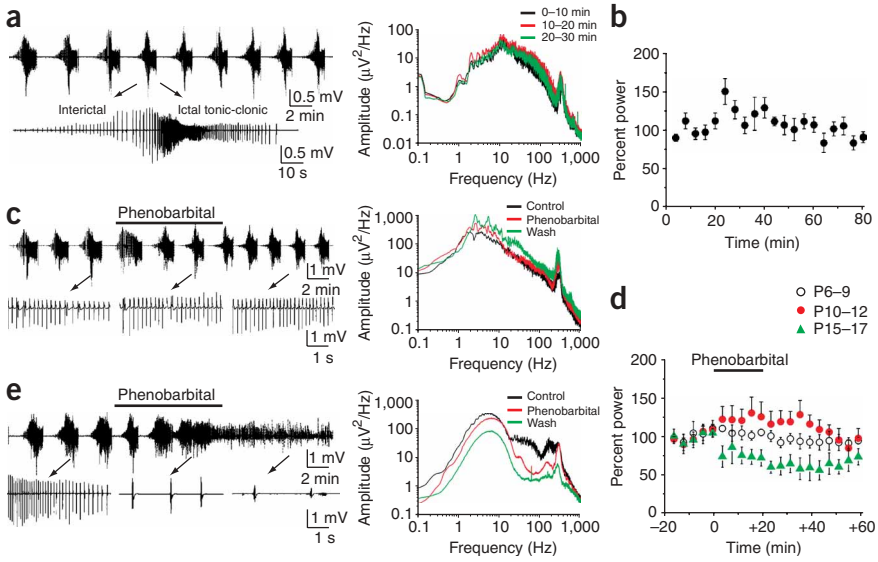

Figure 2 Effects of phenobarbital on epileptiform activity in the neonatal rat hippocampus *in vitro*. (**a**) Extracellular field potential recording of the interictal and ictal-like epileptiform activity induced by 8.5 mM $[K^+]_o$ in the CA3 pyramidal cell layer of P10 rat hippocampal slice. Ictal-tonic episode is shown on an expanded time scale. Right, power spectra of epileptiform activity in consecutive 10-min windows showing similar amplitude in the EEG (1–100 Hz) and fast-ripple (200–400 Hz) frequency range. (**b**) Power of extracellular field activity in consecutive 4-min windows after continuous application of 8.5 mM $[K^+]_o$. Averaged data from 12 recordings in six P10–12 rat hippocampal slices. (**c**) Ictal-tonic discharges in the CA3 pyramidal cell layer of P12 rat hippocampal slice are potentiated by phenobarbital (100 μM), consistent with the lack of efficacy in human neonates. Right, power spectra of epileptiform activity in consecutive 10-min windows before, during and after phenobarbital application. (**d**) Phenobarbital does not depress power of epileptiform activity induced by 8.5 mM $[K^+]_o$ in P6–9 ($n = 6$) and P10–12 ($n = 7$) hippocampal slices. In the hippocampal slices from P15–18 rats, phenobarbital reduced the power of epileptiform activity by 35 ± 8.9% ($n = 6$). (**e**) Phenobarbital (100 μM) depresses epileptiform activity induced by 8.5 mM $[K^+]_o$ in the CA3 pyramidal cell layer of P15 rat hippocampal slice. Right, power spectra of epileptiform activity in consecutive 10-min windows before, during and after phenobarbital application. Phenobarbital depressed the power spectra amplitude.

conductances[32]. Although these compounds are effective anticonvulsants in the more mature brain, the excitatory effects of GABA in immature neurons[12,13] renders these anticonvulsants ineffective[33], as is clear from EEG recordings of treated neonatal seizures[10].

We studied the effects of phenobarbital on recurrent interictal and ictal-like epileptiform activity in the hippocampal slices *in vitro* from P6–20 rats. We performed simultaneous multisite extracellular field potential records in the CA3 pyramidal cell layer. Bath application of 8.5 mM K^+ induced a progressive increase in neuronal firing that developed to recurrent interictal and ictal-like epileptiform activities[14,34] (**Fig. 2a**). Sustained ictal-tonic discharges can be elicited during the P5–17 postnatal period and ictal-clonic discharges can be elicited until end of the third postnatal week[14]. We analyzed the power of extracellular field potential during 8.5 mM K^+–induced epileptiform activity in the 0.1–1,000 Hz frequency band that includes both theta-gamma and fast-ripple oscillations[35]. Power spectra in consecutive 10-min windows showed similar amplitudes in the EEG (1–100 Hz) and fast-ripple (200–400 Hz) frequency ranges (**Fig. 2a**). Over long periods of 8.5 mM K^+ application (60–90 min), the power of epileptiform activity tended to increase during the first 20–40 min and then gradually decrease ($n = 6$; **Fig. 2b**).

Bath application of phenobarbital (100 μM) did not suppress interictal and ictal-like epileptiform activity in hippocampal slices from neonatal (P6–9) rats ($n = 6$) nor from P10–12 rats ($n = 7$; **Fig. 2c,d**). Averaged power of epileptiform activity in control and after phenobarbital application was not significantly different ($P = 0.09$ for P6–9 and $P = 0.06$ for P10–12 rats; **Fig. 2d**). In the hippocampal slices from older (P15–17) rats, phenobarbital abolished ictal-tonic-clonic discharges ($n = 5$ from six slices) and reduced the power of epileptiform activity by 35 ± 8.9% ($n = 6$, $P = 0.002$; **Fig. 2d,e**).

NKCC1 inhibition alters E_{GABA} and network activity

To test the hypothesis that NKCC1 is responsible for the neuronal accumulation of Cl^- [19,21] that causes $GABA_A$ receptor activation to be excitatory in the immature nervous system[12,13], we studied the effect of selective inhibition of NKCC1 by bumetanide[23] on E_{GABA}. We used whole-cell voltage-clamp recordings to measure the reversal potential of conductances elicited by local application of GABA (100 μM, 10–20 ms pulse duration) in P4–6 CA1 pyramidal cells. E_{GABA} was more hyperpolarized in the presence of bumetanide (−40.4 ± 2.7 mV, $n = 6$ cells; $P = 0.005$) than in control (−37 ± 2.7 mV, $n = 8$; **Fig. 3a**). A similar value of E_{GABA} and negative shift in E_{GABA} has been described in immature neocortical neurons, but not mature neurons, using the gramicidin-perforated patch-clamp method[21].

In the immature hippocampus, the excitatory action of GABA contributes to increased excitability and the generation of physiological patterns of spontaneous network-driven activity described as giant depolarizing potentials[36–38]. We observed giant depolarizing potentials in the neonatal rat hippocampus until P12, the same time window in which GABA exerts a depolarizing action[14]. We performed simultaneous whole-cell voltage-clamp recordings of CA3 pyramidal cells and extracellular field potential recordings in CA3 pyramidal cell layer to analyze the effects of bumetanide on spontaneous network activity in the P4–8 hippocampal slices *in vitro* (**Fig. 3b**). Spontaneous neuronal network activity is characterized by large polysynaptic currents that are mediated by activation of $GABA_A$-Rs and by synchronous recurrent population bursts, which are associated with a barrage of high-frequency action potentials from multiple cells. Bath application of bumetanide (10 μM) rapidly depressed synchronous burst of action potentials ($n = 10$). Synchronous network activity reappeared 10–15 min after wash of bumetanide.

NKCC1 facilitates seizures in the developing hippocampus

During development of inhibitory synapses, the action of the neurotransmitter GABA shifts from depolarizing to hyperpolarizing[12,14,15]. The shift results from an age-dependent regulation of the intracellular concentration of free Cl^- in postsynaptic neurons[21]. If the NKCC1 transporter is responsible for accumulation of intracellular Cl^- ($[Cl^-]_i$), the depolarizing action of GABA and the higher propensity for seizures in the neonatal brain, then inhibition of

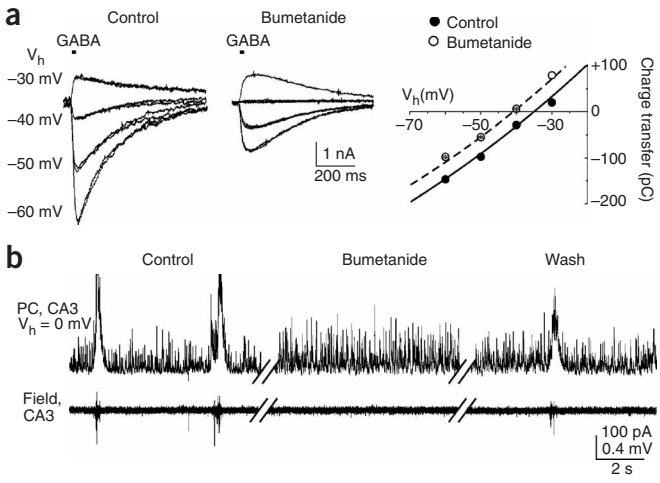

Figure 3 Effects of NKCC1 inhibition on E_{GABA} and spontaneous network activity. (**a**) CA1 pyramidal cell in the 4-d-old rat hippocampal slice was voltage clamped at −60 mV and stepped to different holding potentials (−60 to −30 mV, 10 mV steps). Internal Cl^- concentration ($[Cl^-]_i$) was 20 mM. Superimposed traces represent GABA-induced currents at different command potentials. Bath application of bumetanide (10 μM) resulted in a negative shift of E_{GABA}. Right, corresponding charge transfer-voltage relationship in control and after bumetanide application. (**b**) Simultaneous recordings of a CA3 pyramidal cell (top) and extracellular field potential in CA3 pyramidal cell layer (bottom) in a P5 hippocampal slice. The CA3 pyramidal cell was whole-cell voltage clamped at 0 mV ($[Cl^-]_i$ = 4.2 mM). In the control, activity is characterized by spontaneous polysynaptic currents mediated by activation of $GABA_A$ receptors and synchronous bursts of action potentials. Bath application of bumetanide (10 μM) caused a transient block of synchronous network activity.

NKCC1-mediated Cl^- transport should suppress epileptiform activity in the developing hippocampus.

We tested whether bumetanide would suppress 8.5 mM K^+–induced epileptiform activity in hippocampal slices from P7–23 rats. Bath application of bumetanide (10 μM) strongly suppressed interictal and ictal-like epileptiform activity in P7–9 hippocampal slices ($n = 10$; **Fig. 4a**) and depressed epileptiform activity in P10–12 hippocampal slices ($n = 6$). Averaged power of epileptiform activity was decreased by 71 ± 2.1% in P7–9 rat hippocampal slices ($P = 1.57 \times 10^{-12}$) and by 41.9 ± 1.5% at P10–12 ($P = 2.13 \times 10^{-11}$; **Fig. 4b**). In the hippocampal slices from P15–17 rats bumetanide transiently reduced power of interictal and ictal-like epileptiform activity by 33 ± 11% ($n = 6$, $P = 0.002$; **Fig. 4b**). In the hippocampal slices from mature rats (P21–23), bumetanide did not depress the power of interictal epileptiform activity ($n = 10$, $P = 0.85$; **Fig. 4b,c**).

To assess the specificity of the effects of bumetanide, we tested whether $GABA_A$-R antagonists prevented the effect of bumetanide on power of epileptiform activity in the hippocampal slices from neonatal rats. Bicuculline (10 μM) blocked ictal-like epileptiform activity induced by elevated K^+ in the hippocampal slices from P7–10 rats[14,15] and reduced the power of epileptiform activity by 11.7 ± 2.2% ($n = 6$, $P = 0.006$; **Fig. 4d,e**). In addition, bicuculline reduced the frequency and increased the amplitude of interictal epileptiform discharges (IEDs). Subsequent application of bumetanide (10 μM) in the presence of bicuculline decreased length of IED by 2.2 ± 8% ($n = 6$; $P = 0.8$) and increased frequency of IED by 22.8 ± 6.4% ($P = 0.008$), but did not change the average power of epileptiform discharges ($P = 0.35$; **Fig. 4e**).

Effects of bumetanide in NKCC1-knockout mice

To show that the effects of bumetanide are mediated by inhibition of NKCC1, we tested the effects of bumetanide on epileptiform activity in NKCC1-knockout (*Slc12a2*$^{-/-}$) mice[39,40]. We measured the effects of bumetanide on 8.5 mM $[K^+]_o$–induced epileptiform activity in

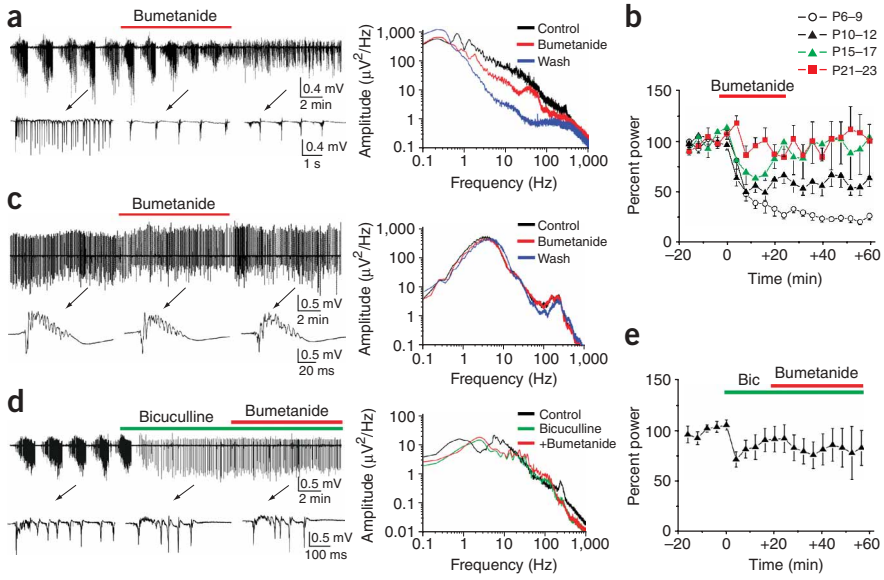

Figure 4 Age-dependent effect of bumetanide on epileptiform activity. (**a**) Left, extracellular field potential recording from the CA3 pyramidal cell layer of P7 rat hippocampal slices in the presence of 8.5 μM $[K^+]_o$. Inhibition of NKCC1-mediated neuronal Cl^- import by bumetanide (10 μM) depressed ictal-like epileptiform activity. Expanded sections of the trace show suppression of ictal-tonic discharges by bumetanide. Right, power spectra of epileptiform activity in 10-min windows before, during and after drug application. Bumetanide strongly depressed the power spectra amplitude. (**b**) Averaged power of epileptiform activity induced by 8.5 mM $[K^+]_o$ before and after bumetanide application. Bumetanide strongly depressed the power of epileptiform activity in P7–9 and P10–12 hippocampal slices but was ineffective in P21-23 slices. (**c**) Left, bumetanide (10 μM) did not depress interictal epileptiform discharges (IEDs) in P22 rat hippocampal slices. Examples of IEDs before, during and after bumetanide application are shown on an expanded time scale. Right, power spectra of epileptiform activity in 10-min windows before, during and after drug application. (**d**) Left, in a P10 hippocampal slice, the $GABA_A$-R antagonist bicuculline (10 μM) blocked ictal-like activity and abolished the anticonvulsant effect of bumetanide. Bumetanide (10 μM) was applied in the presence of bicuculline. Examples of ictal-tonic discharges before bicuculline application and interictal epileptiform discharges before and after bumetanide application are shown on an expanded time scale. Right, power spectra of epileptiform activity in 10-min windows before and during drug applications. (**e**) Power of 8.5 mM $[K^+]_o$ induced epileptiform activity is not affected by bumetanide in the presence of bicuculline (Bic).

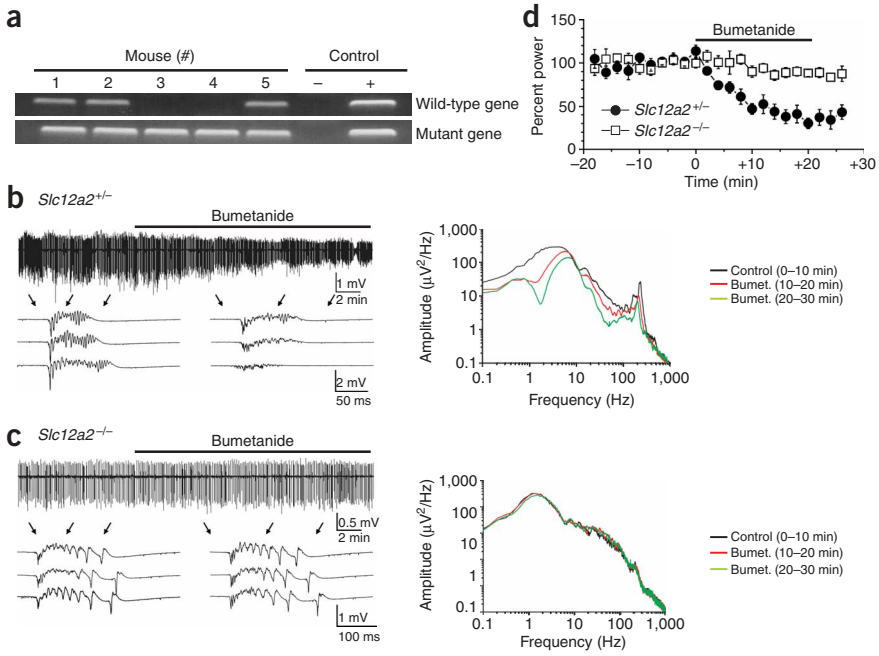

Figure 5 Effects of bumetanide in *Slc12a2*$^{-/-}$ mice. (**a**) Confirmation of two *Slc12a2*$^{-/-}$ mice by PCR. (**b**) Bumetanide (10 μM) depressed interictal epileptiform activity induced by 8.5 mM $[K^+]_o$ in P9 control mouse (#5) hippocampal slices *in vitro*. Expansion of sections of the traces shows suppression of interictal epileptiform discharges (IEDs) by bumetanide in this extracellular field potential recording from the CA3 pyramidal cell layer. Right, log plots of power spectra of epileptiform activity in 10-min windows before and after bumetanide application. Bumetanide strongly depressed the power spectra amplitude. (**c**) Bumetanide (10 μM) did not depress interictal epileptiform activity induced by 8.5 mM $[K^+]_o$ in P8 *Slc12a2*$^{-/-}$ mouse (#3) hippocampal slices *in vitro*. Expansion of the traces show IEDs before and after bumetanide application in this extracellular field potential recording from the CA3 pyramidal cell layer. Right, log plots of power spectra of epileptiform activity in 10-min windows before and after bumetanide application. (**d**) Averaged power of epileptiform activity after bumetanide application in *Slc12a2*$^{+/-}$ ($n = 8$) and *Slc12a2*$^{-/-}$ ($n = 10$) mouse hippocampal slices.

hippocampal slices prepared from P7–9 *Slc12a2*$^{-/-}$ mice versus *Slc12a2*$^{+/-}$ control littermates (**Fig. 5a**). Simultaneous multisite extracellular field potential recordings in the CA3 pyramidal cell layer showed that bath application of 8.5 mM K^+ induced a progressive increase in neuronal firing that developed into interictal epileptiform discharges. Bath application of bumetanide (10 μM) strongly depressed the amplitude and duration of interictal epileptiform discharges in hippocampal slices from heterozygous mice ($n = 8$ slices from three mice; **Fig. 5b**) and did not change the amplitude and duration of IEDs in hippocampal slices from homozygous mice ($n = 10$ slices from two mice; **Fig. 5c**). The averaged power of epileptiform activity after bumetanide application in *Slc12a2*$^{+/-}$ mouse hippocampal slices was decreased by 51 ± 4.7% ($P = 1.7 \times 10^{-8}$; **Fig. 5d**) and was not significantly changed in *Slc12a2*$^{-/-}$ mouse hippocampal slices ($P = 0.056$; **Fig. 5d**).

Ictal tonic-clonic seizures in neonatal rats *in vivo*

To test whether inhibition of NKCC1 would suppress seizures *in vivo*, we studied seizures in rat pups. Two days after implantation of recording electrodes, six P9–10 rats received subcutaneous injection with kainic acid (2 mg/kg) and six P9–10 control rats received subcutaneous 0.9% sodium chloride saline injections. Ten to twenty minutes after kainic acid injection, a regular pattern of behavioral signs emerged, involving scratching-like movements of the hindpaws, loss of balance and turning on the side (**Fig. 6a**). Recurrent interictal and ictal EEG patterns occurred 20–80 min (61.2 ± 10.4 min; mean ± s.e.m.) after kainic acid injection in all rats from this experimental group (**Fig. 6b**). We observed no behavioral or EEG seizures in the control rats. Interictal spikes usually occurred synchronously in the left and right hemispheres (**Fig. 6c**). Frequency of the interictal spikes was 1.43 ± 0.06 Hz ($n = 23$ seizures in six rats). Before transition to ictal patterns, interictal spikes were usually followed by fast-ripple (100–500 Hz) and gamma-frequency oscillations (20–50 Hz). Tonic-clonic seizures were the most common type of seizures induced by kainic acid in P9–10 rats. The ictal-tonic phase lasted 12.6 ± 1.4 s (16 seizures in five rats). Population spikes of 18.7 ± 1.2 Hz were characteristic of the tonic phase of kainate acid–induced seizures (**Fig. 6c**). Tonic discharges were followed by clonic bursts (**Fig. 6c**). Large-amplitude population spikes followed by 100–200 Hz ripples and 200–1,200 ms gamma-frequency afterdischarges characterized the clonic bursts. The mean duration of the clonic phase was 36.4 ± 5 s (25 seizures in six rats). The ictal patterns were followed by postictal depression (**Fig. 6b,c**). During ictal EEG activity, motor activity consisted of scratching, jerky movements, turning on the side or on the back and frequent tail shaking. Five to ten recurrent seizures with an average interval 379 ± 24.5 s were followed by periodic epileptiform discharges (**Fig. 6b,c**).

Bumetanide for neonatal seizure therapy

Two days after implantation of recording electrodes, 22 P9–12 age-matched rats received subcutaneous injection with kainic acid (2 mg/kg). Ten minutes after kainic acid injection, ten rats received intraperitoneal injection of 0.9% sodium chloride saline, six rats received intraperitoneal phenobarbital (25 mg/kg) and six rats received intraperitoneal bumetanide (0.1–0.2 mg/kg). We compared patterns and power of EEG activity in these three groups of rats (**Fig. 6d–f**).

After kainic acid and sodium chloride saline injections, recurrent interictal and ictal-clonic EEG activity occurred in all rats in this experimental group (100%). The frequency of interictal spikes was 1.4 ± 0.1 s ($n = 33$ seizures in 10 rats). The mean duration of single ictal episode including interictal and ictal phases was 96.8 ± 8.6 s ($n = 38$ seizures in 10 rats). The mean interval between seizures was 323 ± 23 s. In eight of ten rats (80%), seizures included 18.2 ± 1.1 Hz tonic discharges lasting 11.9 ± 1.3 s ($n = 23$ seizures). The ictal-clonic pattern lasting 40.3 ± 5.1 s ($n = 38$) was characterized by primary population spikes followed by secondary afterdischarges. The average power of the EEG activity in 2-min windows after seizure onset was 2,186.4 ± 110.7 μV^2 ($n = 12$ recordings in six rats).

In the six rats in which kainic acid injection was followed by phenobarbital injection, all developed recurrent interictal and ictal-clonic activity (100%). The interictal phase was characterized by population spikes at 1.6 ± 0.1 Hz, followed by gamma-frequency

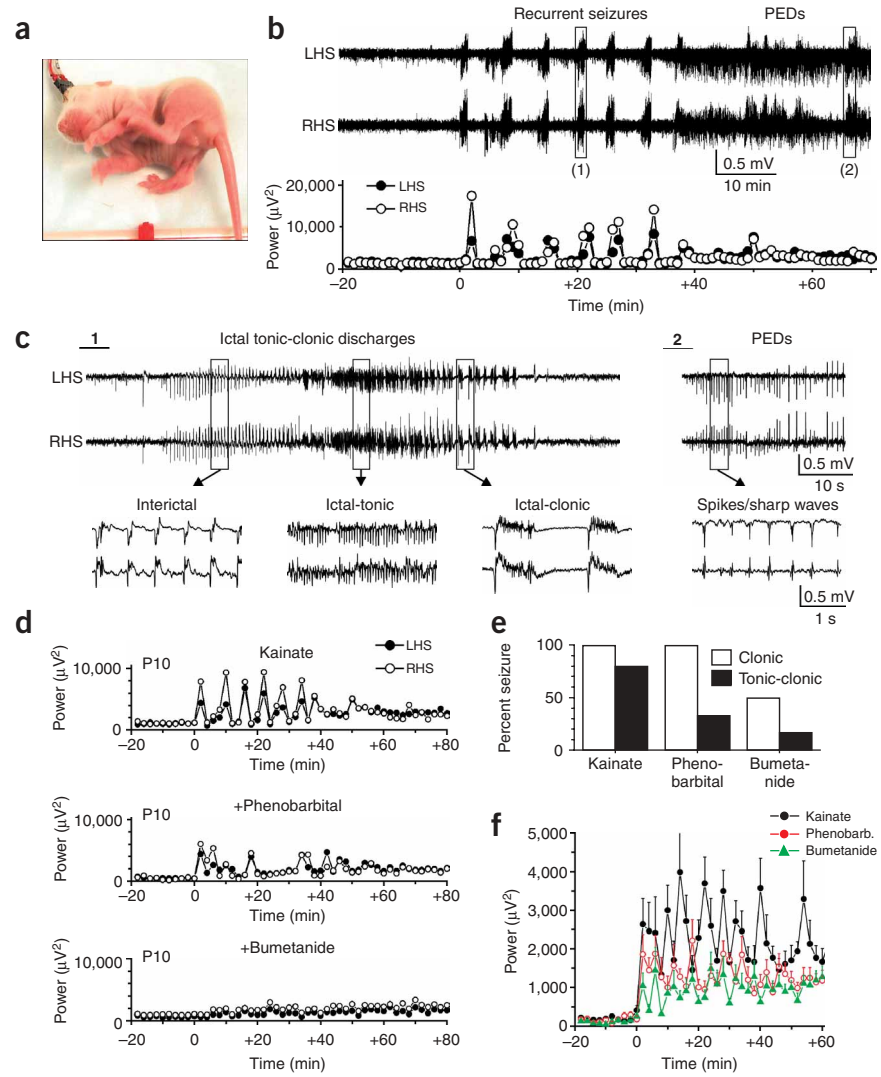

Figure 6 Bumetanide for neonatal seizure therapy. (**a**) Photograph of implanted neonatal (P10) rat during kainic acid–induced seizures. (**b**) Continuous EEG recordings from the left and right hemispheres (LHS and RHS) in a P10 rat show recurrent tonic-clonic seizures followed by periodic epileptiform discharges (PEDs). Bottom, corresponding power of EEG activity in sequential 1-min windows shows periodic peaks corresponding to the ictal tonic-clonic episodes. Filled and open circles indicate the power of EEG signals from the left and right hemispheres, respectively. (**c**) Example of tonic-clonic seizures and PEDs (expanded from boxes 1 and 2 in **b**) and further expansions showing interictal, tonic and clonic discharges are shown on an expanded time scale. (**d**) Power of EEG activity in 2-min windows preceding kainate acid–induced seizures and after onset of seizures (time 0) in the P10 rats *in vivo*. Intraperitoneal administration of phenobarbital (25 mg/kg) or bumetanide (0.1–0.2 mg/kg) preceding onset of kainate acid–induced seizures depressed power of transient epileptic state. Data are from three randomly selected rats. Filled and open circles correspond to power of EEG signals recorded from the left and right hemispheres, respectively. (**e**) Group data of the kainate acid–induced epileptiform activity after injection of 0.9% sodium chloride, phenobarbital or bumetanide. Filled and open columns correspond to the ictal-clonic and ictal tonic-clonic activities, respectively. (**f**) Power of EEG activity averaged over 2-min windows before kainate acid–induced seizures and after onset of seizures (time 0) in P10–12 rats ($n = 6$) *in vivo*. Compared to vehicle controls (black circles), the average power of epileptiform activity was 40% lower ($n = 6$; $P = 2.1 \times 10^{-10}$) in the presence of phenobarbital (red circles) and 51% lower ($n = 6$; $P = 9.1 \times 10^{-4}$) in the presence of bumetanide (green triangles).

afterdischarges before transition to ictal-clonic phase. The mean duration of single ictal episode was 27.4 ± 2.6 s ($n = 19$). The mean interval between seizures was 241.3 ± 45.8 s. The ictal-tonic pattern lasting 5.2 ± 1.4 s ($n = 4$ seizures) occurred in two rats (33.3%; $n = 2$ of 6). The frequency of the ictal-tonic discharges was 14 ± 3 Hz. The ictal-clonic pattern lasting 12 ± 1.1 s ($n = 19$) was characterized by primary population spikes followed by secondary afterdischarges. The averaged power of EEG activity in 2-min windows after seizure onset was 1,309.9 ± 48.3 μV^2 ($n = 12$ recordings in six rats), suggesting that phenobarbital depressed kainic acid–induced epileptiform activity by 40.4% ($P = 2.1 \times 10^{-10}$).

After kainic acid and subsequent bumetanide injection, periodic epileptiform discharges occurred in all six rats. We observed that three rats from this experimental group had EEG clonic seizures (50%). One rat from these three also had tonic-clonic seizures (16.7%). The frequency of interictal spikes preceding transition to ictal activity was 1.4 ± 0.1 Hz (12 seizures). The mean duration of seizure including interictal and ictal phases was 32 ± 3.9 s ($n = 12$ seizures in three rats). The ictal-tonic phase lasted 9 ± 1.9 s ($n = 4$ seizures in one rat) and ictal-clonic phase 12.5 ± 1.1 s ($n = 12$ seizures in three rats). The mean interval between recurrent seizures was 360.1 ± 68.6 s. Averaged power of EEG activity in 2-min windows after seizure onset was 1,066 ± 49.2 μV^2 ($n = 12$ recordings in six rats), suggesting that bicuculline depressed kainic acid–induced epileptiform activity by 51.2% ($P = 3.6 \times 10^{-14}$). The effect of bumetanide was significantly different from the effect of phenobarbital ($P = 9.1 \times 10^{-4}$; one-way ANOVA test).

Comparison of these three experimental groups provides clear evidence for the potential anticonvulsant application of the diuretic bumetanide to improve the therapy of neonatal seizures.

DISCUSSION

In the rodent, Cl^- transporters are known to be developmentally regulated: NKCC1 expression in cortical neurons is highest during the first postnatal week, and then decreases from P14 to the low levels found in adults. KCC2 is minimal at birth, low during the first postnatal week and comparable with adult at P14–15. The ontogeny of these Cl^- transporters has been studied by PCR and *in situ* hybridization[16,21,24,25,41], whole-forebrain western blots and immunocytochemistry[24,30]. In the rat, the expression of NKCC1 correlates with high intracellular Cl^- concentration[21,42] and with depolarizing effect of GABA[12–15]. Our data show for the first time that a similar expression pattern is present in human, with high neuronal expression of NKCC1 and low expression of KCC2 in the neonate and before the

end of the first year of life. These data strongly support the hypothesis that human neonatal seizures are poorly responsive to GABAergic anticonvulsants because of immature Cl^- transport patterns and suggest that the anticonvulsant action of bumetanide should be as effective in the immature human brain as it is in the immature rat brain.

Here we also show that inhibition of the Cl^- transporter NKCC1 by bumetanide produces a negative shift in the $GABA_A$ reversal potential, inhibits synchronous network activity in perinatal hippocampus that is dependent on GABA-mediated excitation, suppresses interictal and ictal-like activity in perinatal hippocampal slices *in vitro* and attenuates kainate-induced seizure activity *in vivo*. The anticonvulsant effects of bumetanide were blocked by a $GABA_A$-R antagonist, indicating that bumetanide is acting through the $GABA_A$-R signaling pathway. The concentrations of bumetanide used in this study selectively inhibit NKCC1 (ref. 23), and bumetanide had no effect on epileptiform activity in brain slices from *Slc12a2*$^{-/-}$ mice, indicating that inhibition of this Cl^- accumulation pathway is the mechanism by which bumetanide exerts its GABA-dependent anticonvulsant effects.

Our study used EEG rather than behavioral measures of seizures. Congruent with the finding that neuronal Cl^- transport matures in a caudal-rostral pattern[16], GABAergic anticonvulsants inhibit motor manifestations of neonatal seizures much more than cortical EEG activity[10,11]. Inhibition of motor manifestations of seizures is beneficial in that it reduces the metabolic cost of seizure activity. But ample scientific data highlight the deleterious effects of EEG neonatal seizures on future cognition and seizure threshold[6–8].

Although our *in vivo* experiments show a clear therapeutic effect of bumetanide on neonatal seizures, it should be kept in mind that the youngest age at which the EEG could be recorded was P9, at which time NKCC1 activity is already declining. More compelling effects are likely to be seen in less mature subjects.

EEG seizures respond poorly to anticonvulsant drugs in the neonatal period. This is not unexpected based on the anticonvulsant drugs most commonly used (phenobarbital and benzodiazepines), the mechanism of action of these drugs (prolongation of $GABA_A$-R open time)[32], and the excitatory action of GABA in the immature nervous system[13,14]. The excitatory action of GABA in the immature nervous system depends on intracellular accumulation of Cl^- through NKCC1 (ref. 21) so that when the $GABA_A$-Rs are activated, Cl^- leaves the neuron, depolarizing the membrane potential[12–15]. In contrast, adult cortical neurons actively export Cl^- through KCC2 so that $GABA_A$-R activation leads to net influx of Cl^-, hyperpolarizing the neuronal membrane and reducing firing[20]. The $GABA_A$ reversal potential can be slightly positive to membrane potential and $GABA_A$ receptor activation can still inhibit the neuron by virtue of shunting more strongly depolarizing conductances[43]. Thus, to render GABA inhibitory in the immature brain, it should not be necessary to initiate active export of Cl^-; rather, inhibition of active import of Cl^- should be sufficient to limit $GABA_A$-R–mediated excitation.

We found that selective inhibition of NKCC1 by bumetanide increased the inhibitory action of $GABA_A$-R activation in the immature nervous system, and had anticonvulsant effects that were substantially better than phenobarbital. GABA-mediated excitation resulting from neuronal accumulation of Cl^- contributes to the lower seizure threshold in the immature nervous system[14], and our study provides evidence that this accumulation of Cl^- is mediated by NKCC1 (ref. 21) because of the effects of low concentrations of bumetanide, the lack of effect of bumetanide in *Slc12a2*$^{-/-}$ mice and the high levels of NKCC1 expression in the neonatal period. Inhibition of NKCC1 causes E_{GABA} to be more negative, and seems to be the anticonvulsant mechanism of bumetanide in the neonate.

The bumetanide-induced shift we measured in E_{GABA} was fairly modest in comparison to the substantial changes in network activity induced by bumetanide. This probably reflects a prolonged decay of intracellular stores of Cl^- in a slice preparation that is relatively inactive compared to *in vivo*, and particularly compared to *in vivo* seizure activity. At higher levels of GABA-mediated synaptic activity, chloride stores will drop more rapidly, and there will be a correspondingly larger change in E_{GABA}. Other groups have shown that transport of Cl^- can be substantially altered with only minor changes in resting E_{GABA} in the slice preparation[44].

High concentrations of diuretic drugs have been shown to have anticonvulsant activity experimentally[45,46], and lower concentrations have recently been shown to block interictal activity *in vivo*[47]. Epidemiological studies have also provided evidence that diuretic drugs have anticonvulsant effects at clinically relevant dosages in adults with epilepsy[48]. It has recently been shown that subicular neurons from individuals with intractable seizures accumulate Cl^- such that $GABA_A$-R activation is excitatory[49], and neurons in experimental epilepsy models have reduced export of Cl^-[44]. These findings suggest that inhibition of NKCC1 might also mediate the anticonvulsant effects of diuretic drugs in some types of seizures in the mature nervous system.

The pharmacokinetics of bumetanide have been studied in the human neonate[28,29], and current anticonvulsant therapy for neonatal seizures is ineffective[10,11]. We show that bumetanide inhibits NKCC1 and suppresses seizures at dosages already tested for diuretic effects[23]. Bumetanide therapy may therefore be useful in the treatment of neonatal seizures.

METHODS

Animals. We housed rats in a temperature-controlled animal-care facility with a 12-h light-dark cycle. All procedures were approved and in accordance with the guidelines of institutional Animal Care and Use Committee and the National Institutes of Health Guide for the Care and Use of Laboratory Animals. We made all efforts to minimize animal suffering and the number of animal used.

Human subjects. We obtained human parietal lobe autopsy specimens from Children's Hospital and Brigham and Women's Hospital, Boston, and University of Maryland Brain Tissue Bank for Developmental Disorders. All specimens were collected under guidelines approved by the hospitals' Institutional Review Boards. Cases included in this study were selected based on combined clinical criteria (cause of death, survival interval and postmortem interval) and neuropathological analysis (**Supplementary Methods** online).

Western blot analysis. Long Evans rats were killed at P3–P21 and at adulthood ($n = 14$). We quickly removed brains and separated frontal-parietal cortex specimens, rapidly froze them in ethanol and stored them at −80 °C until they were used for protein extraction. Human parietal lobe specimens ranging from 20 PCW (gestational plus postnatal weeks) to 57 years ($n = 12$) were removed in blocks at the time of autopsy, snap-frozen immediately and stored at −80 °C. Subsequently, we separated gray matter and used samples for protein extraction. We processed rat and human tissue samples using the same protocol (**Supplementary Methods** online).

Immunocytochemistry. Long Evans rats were killed at P3–P21 ($n = 13$). We deeply anesthetized the rats (50–100 mg/kg pentobarbital intraperitoneally, depending on postnatal age) and perfused them intracardially with 0.1 M PBS, followed by 4% paraformaldehyde in PBS (pH 7.4). We subsequently removed brains, postfixed them at room temperature for 4 h in the same paraformaldehyde-containing solution and cryoprotected them in 30% sucrose overnight.

We collected coronal sections, cut at 50 μm on a freezing microtome, serially and maintained them in 0.1% sodium azide in PBS at 4 °C until use. We fixed human frozen parietal lobe specimens, ranging from 31–210 PCW (n = 6) in a precooled paraformaldehyde-containing solution for 1 week at −20 °C and then cryoprotected them in 30% sucrose in PBS for 24 h. The fixative contained: 12 g paraformaldehyde and 40 g sucrose in 100 ml 0.1 M PBS, 40 ml 100% ethanol, 40 ml 100% ethylene glycol and 20 ml 100% glycerol[50]. Sections were similarly cut on a freezing microtome at 80–100 μm, collected serially and maintained in 0.1% sodium azide in PBS at 4 °C until use. We used the same immunostaining protocol for both rat and human tissue sections (**Supplementary Methods** online).

Genotyping. We obtained *Slc12a2*$^{-/-}$ mice by deleting exon 9 of the gene encoding the Na^+-K^+-$2Cl^-$ cotransporter and replacing it with a β-galactosidase–neomycin fusion cassette[39]. We performed genotyping using PCR on tail DNA (**Supplementary Methods** online).

Slice preparation for electrophysiology. We performed experiments on hippocampal slices prepared from male Wistar rats at P5–23, as well as P7–9 C57 black mice. We prepared slices as described previously[14,34] (**Supplementary Methods** online).

***In vitro* recordings.** For electrophysiological recordings, we transferred individual slices to a conventional submerged-type chamber and continuously superfused them with oxygenated artificial cerebrospinal fluid at 32 °C and at a rate of 2–3 ml/min. We performed recordings as described previously[14,34] (**Supplementary Methods** online).

***In vivo* recordings.** We implanted male Wistar rats with parietal EEG electrodes at P7–8. We amplified wide-band EEG signals through a direct current–coupled amplifier and analyzed them as described in **Supplementary Methods** online. We administered kainic acid (2 mg/kg), a glutamate receptor agonist, subcutaneously. We injected bumetanide (0.1–0.2 mg/kg), phenobarbital (25 mg/kg) or 0.9% sodium chloride intraperitoneally 10–15 min after kainic acid administration, before seizure onset.

Drugs. We purchased reagents from Sigma-RBI and Tocris, prepared them as stock solutions and stored them as aliquots in tightly sealed vials at the manufacturers' recommended temperatures. During the experiments, we kept thawed aliquots on ice and protected them from light until use.

Statistical analysis. Group measures are expressed as mean ± s.e.m.; error bars also indicate s.e.m. We assessed the statistical significance of differences between control and experimental conditions with the Student *t*-test. We used one-way analysis of variances (ANOVA) test to ascertain the differences between two or more drug effects. The level of significance was set at $P < 0.05$.

Note: Supplementary information is available on the Nature Medicine website.

ACKNOWLEDGMENTS

This work was supported by the US National Institutes of Health and National Institute of Neurological Disorders and Stroke grants NS34360, NS34700, and NS40109 (to K.J.S.), NS36758 (to E.D.), NS31718 (to F.E.J.), NS38475 (to F.E.J. and D.M.T.) and the Hearst Foundation (to D.M.T.). Some tissue samples were provided by the University of Maryland Brain Tissue Bank for Developmental Disorders, Baltimore, Maryland, USA supported by N01-HD-43368.

COMPETING INTERESTS STATEMENT

The authors declare that they have no competing financial interests.

Published online at http://www.nature.com/naturemedicine/
Reprints and permissions information is available online at http://npg.nature.com/reprintsandpermissions/

1. Ronen, G.M., Penney, S. & Andrews, W. The epidemiology of clinical neonatal seizures in Newfoundland: a population-based study. *J. Pediatr.* **134**, 71–75 (1999).
2. Painter, M.J., Bergman, I. & Crumrine, P. Neonatal seizures. *Pediatr. Clin. North Am.* **33**, 91–109 (1986).
3. Scher, M.S. *et al.* Electrographic seizures in preterm and full-term neonates: clinical correlates, associated brain lesions, and risk for neurologic sequelae. *Pediatrics* **91**, 128–134 (1993).
4. Brunquell, P.J., Glennon, C.M., DiMario, F.J. Jr., Lerer, T. & Eisenfeld, L. Prediction of outcome based on clinical seizure type in newborn infants. *J. Pediatr.* **140**, 707–712 (2002).
5. Jensen, F.E., Holmes, G.L., Lombroso, C.T., Blume, H.K. & Firkusny, I.R. Age-dependent changes in long-term seizure susceptibility and behavior after hypoxia in rats. *Epilepsia* **33**, 971–980 (1992).
6. Baram, T.Z. Long-term neuroplasticity and functional consequences of single versus recurrent early-life seizures. *Ann. Neurol.* **54**, 701–705 (2003).
7. Holmes, G.L. Effects of early seizures on later behavior and epileptogenicity. *Ment. Retard. Dev. Disabil. Res. Rev.* **10**, 101–105 (2004).
8. Swann, J.W. The impact of seizures on developing hippocampal networks. *Prog. Brain Res.* **147**, 347–354 (2005).
9. Sanchez, R.M., Dai, W., Levada, R.E., Lippman, J.J. & Jensen, F.E. AMPA/kainate receptor-mediated downregulation of GABAergic synaptic transmission by calcineurin after seizures in the developing rat brain. *J. Neurosci.* **25**, 3442–3451 (2005).
10. Connell, J., Oozeer, R., de Vries, L., Dubowitz, L.M. & Dubowitz, V. Clinical and EEG response to anticonvulsants in neonatal seizures. *Arch. Dis. Child.* **64**, 459–464 (1989).
11. Painter, M.J. *et al.* Phenobarbital compared with phenytoin for the treatment of neonatal seizures. *N. Engl. J. Med.* **341**, 485–489 (1999).
12. Owens, D.F. & Kriegstein, A.R. Is there more to GABA than synaptic inhibition? *Nat. Rev. Neurosci.* **3**, 715–727 (2002).
13. Ben Ari, Y. Excitatory actions of gaba during development: the nature of the nurture. *Nat. Rev. Neurosci.* **3**, 728–739 (2002).
14. Dzhala, V.I. & Staley, K.J. Excitatory actions of endogenously released GABA contribute to initiation of ictal epileptiform activity in the developing hippocampus. *J. Neurosci.* **23**, 1840–1846 (2003).
15. Khazipov, R. *et al.* Developmental changes in GABAergic actions and seizure susceptibility in the rat hippocampus. *Eur. J. Neurosci.* **19**, 590–600 (2004).
16. Stein, V., Hermans-Borgmeyer, I., Jentsch, T.J. & Hubner, C.A. Expression of the KCl cotransporter KCC2 parallels neuronal maturation and the emergence of low intracellular chloride. *J. Comp. Neurol.* **468**, 57–64 (2004).
17. Scher, M.S., Alvin, J., Gaus, L., Minnigh, B. & Painter, M.J. Uncoupling of EEG-clinical neonatal seizures after antiepileptic drug use. *Pediatr. Neurol.* **28**, 277–280 (2003).
18. Staley, K., Smith, R., Schaack, J., Wilcox, C. & Jentsch, T.J. Alteration of GABAA receptor function following gene transfer of the CLC-2 chloride channel. *Neuron* **17**, 543–551 (1996).
19. Delpire, E. Cation-chloride cotransporters in neuronal communication. *News Physiol. Sci.* **15**, 309–312 (2000).
20. Payne, J.A., Rivera, C., Voipio, J. & Kaila, K. Cation-chloride co-transporters in neuronal communication, development and trauma. *Trends Neurosci.* **26**, 199–206 (2003).
21. Yamada, J. *et al.* Cl- uptake promoting depolarizing GABA actions in immature rat neocortical neurones is mediated by NKCC1. *J. Physiol. (Lond.)* **557**, 829–841 (2004).
22. Isenring, P., Jacoby, S.C., Payne, J.A. & Forbush, B. III. Comparison of Na-K-Cl cotransporters. NKCC1, NKCC2, and the HEK cell Na-L-Cl cotransporter. *J. Biol. Chem.* **273**, 11295–11301 (1998).
23. Hannaert, P., Alvarez-Guerra, M., Pirot, D., Nazaret, C. & Garay, R.P. Rat NKCC2/NKCC1 cotransporter selectivity for loop diuretic drugs. *Naunyn Schmiedebergs Arch. Pharmacol.* **365**, 193–199 (2002).
24. Plotkin, M.D., Snyder, E.Y., Hebert, S.C. & Delpire, E. Expression of the Na-K-2Cl cotransporter is developmentally regulated in postnatal rat brains: a possible mechanism underlying GABA's excitatory role in immature brain. *J. Neurobiol.* **33**, 781–795 (1997).
25. Wang, C. *et al.* Developmental changes in KCC1, KCC2, and NKCC1 mRNA expressions in the rat brain. *Brain Res. Dev. Brain Res.* **139**, 59–66 (2002).
26. Clayton, G.H., Owens, G.C., Wolff, J.S. & Smith, R.L. Ontogeny of cation-Cl– cotransporter expression in rat neocortex. *Brain Res. Dev. Brain Res.* **109**, 281–292 (1998).
27. Rivera, C. *et al.* The K+/Cl- co-transporter KCC2 renders GABA hyperpolarizing during neuronal maturation. *Nature* **397**, 251–255 (1999).
28. Sullivan, J.E., Witte, M.K., Yamashita, T.S., Myers, C.M. & Blumer, J.L. Pharmacokinetics of bumetanide in critically ill infants. *Clin. Pharmacol. Ther.* **60**, 405–413 (1996).
29. Lopez-Samblas, A.M., Adams, J.A., Goldberg, R.N. & Modi, M.W. The pharmacokinetics of bumetanide in the newborn infant. *Biol. Neonate* **72**, 265–272 (1997).
30. Lu, J., Karadsheh, M. & Delpire, E. Developmental regulation of the neuronal-specific isoform of K-Cl cotransporter KCC2 in postnatal rat brains. *J. Neurobiol.* **39**, 558–568 (1999).
31. Sankar, R. & Painter, M.J. Neonatal seizures: after all these years we still love what doesn't work. *Neurology* **64**, 776–777 (2005).
32. Twyman, R.E., Rogers, C.J. & Macdonald, R.L. Differential regulation of gamma-aminobutyric acid receptor channels by diazepam and phenobarbital. *Ann. Neurol.* **25**, 213–220 (1989).
33. Staley, K. Enhancement of the excitatory actions of GABA by barbiturates and benzodiazepines. *Neurosci. Lett.* **146**, 105–107 (1992).
34. Dzhala, V.I. & Staley, K.J. Transition from interictal to ictal activity in limbic networks *in vitro*. *J. Neurosci.* **23**, 7873–7880 (2003).
35. Dzhala, V.I. & Staley, K.J. Mechanisms of fast ripples in the hippocampus. *J. Neurosci.* **24**, 8896–8906 (2004).
36. Ben Ari, Y., Cherubini, E., Corradetti, R. & Gaiarsa, J.L. Giant synaptic potentials in immature rat CA3 hippocampal neurones. *J. Physiol. (Lond.)* **416**, 303–325 (1989).
37. Khalilov, I., Dzhala, V., Ben Ari, Y. & Khazipov, R. Dual role of GABA in the neonatal rat hippocampus. *Dev. Neurosci.* **21**, 310–319 (1999).

38. Leinekugel, X. *et al.* Correlated bursts of activity in the neonatal hippocampus *in vivo*. *Science* **296**, 2049–2052 (2002).
39. Delpire, E., Lu, J., England, R., Dull, C. & Thorne, T. Deafness and imbalance associated with inactivation of the secretory Na-K-2Cl co-transporter. *Nat. Genet.* **22**, 192–195 (1999).
40. Sung, K.W., Kirby, M., McDonald, M.P., Lovinger, D.M. & Delpire, E. Abnormal GABAA receptor-mediated currents in dorsal root ganglion neurons isolated from Na-K-2Cl cotransporter null mice. *J. Neurosci.* **20**, 7531–7538 (2000).
41. Kanaka, C. *et al.* The differential expression patterns of messenger RNAs encoding K-Cl cotransporters (KCC1,2) and Na-K-2Cl cotransporter (NKCC1) in the rat nervous system. *Neuroscience* **104**, 933–946 (2001).
42. Owens, D.F., Boyce, L.H., Davis, M.B. & Kriegstein, A.R. Excitatory GABA responses in embryonic and neonatal cortical slices demonstrated by gramicidin perforated-patch recordings and calcium imaging. *J. Neurosci.* **16**, 6414–6423 (1996).
43. Staley, K.J. & Mody, I. Shunting of excitatory input to dentate gyrus granule cells by a depolarizing GABAA receptor-mediated postsynaptic conductance. *J. Neurophysiol.* **68**, 197–212 (1992).
44. Jin, X., Huguenard, J.R. & Prince, D.A. Impaired Cl− extrusion in layer V pyramidal neurons of chronically injured epileptogenic neocortex. *J. Neurophysiol.* **93**, 2117–2126 (2005).
45. Hochman, D.W., Baraban, S.C., Owens, J.W. & Schwartzkroin, P.A. Dissociation of synchronization and excitability in furosemide blockade of epileptiform activity. *Science* **270**, 99–102 (1995).
46. Stringer, J.L. & Pan, E. Effect of seizures and diuretics on the osmolality of the cerebrospinal fluid. *Brain Res.* **745**, 328–330 (1997).
47. Haglund, M.M. & Hochman, D.W. Furosemide and mannitol suppression of epileptic activity in the human brain. *J. Neurophysiol.* **94**, 907–918 (2005).
48. Hesdorffer, D.C., Stables, J.P., Hauser, W.A., Annegers, J.F. & Cascino, G. Are certain diuretics also anticonvulsants? *Ann. Neurol.* **50**, 458–462 (2001).
49. Cohen, I., Navarro, V., Clemenceau, S., Baulac, M. & Miles, R. On the origin of interictal activity in human temporal lobe epilepsy *in vitro*. *Science* **298**, 1418–1421 (2002).
50. Ulfig, N., Nickel, J. & Bohl, J. Monoclonal antibodies SMI 311 and SMI 312 as tools to investigate the maturation of nerve cells and axonal patterns in human fetal brain. *Cell Tissue Res.* **291**, 433–443 (1998).